IEICE TRANSACTIONS

on Fundamentals of Electronics, Communications and Computer Sciences

DOI:10.1587/transfun.2024SMP0002

Publicized:2024/09/20

This advance publication article will be replaced by the finalized version after proofreading.

A PUBLICATION OF THE ENGINEERING SCIENCES SOCIETY

The Institute of Electronics, Information and Communication Engineers

Kikai-Shinko-Kaikan Bldg., 5-8, Shibakoen 3 chome, Minato-ku, TOKYO, 105-0011 JAPAN

PAPER

Lightness Modification of Color Image for Protanopia/Deuteranopia in RGB Color Space

Ayaka FUJITA[†], ***Student Member***, **Mashiho MUKAIDA**[††], **Tadahiro AZETSU**[†††], ***Members***, ***and*** **Noriaki SUETAKE**[†], ***Senior Member***

SUMMARY In this paper, we propose a method which converts an original image into the image that does not give a strange impression to trichromatic vision and is easy for dichromatic vision to discriminate colors by modifying only the lightness in the RGB color space, where the color gamut can be easily grasped. In the proposed method, the lightness modification is executed by adding the red-green component multiplied by a coefficient derived from an optimization problem into the lightness component for each pixel. The optimization problem is defined as the minimization of the lightness difference between pixels considering the difference in color. The effectiveness of the proposed method is illustrated through comparison with conventional methods.

key words: *protanopia, deuteranopia, undiscriminatable color, RGB color space, lightness modification, minimization problem*

1. Introduction

Humans have the photoreceptor cells, which are classified into rods and cones, in the deepest part of the retina. There are three types of cones with different spectral sensitivities [1]. These are classified into L, M, and S cones, which respond strongly to the light of long, medium, and short wavelengths, respectively. Humans discriminate colors according to the ratio of response values of these three types of cones. That is, all colors perceived by humans can be represented by a mixture of the three primary colors corresponding to these cones, which is called trichromatic vision [2].

Meanwhile, when the function of each cone is altered due to genetic mutations, color vision changes. Dichromatic vision is a color vision characteristic in which one of the three types of cones is deficient or dysfunctional. This is called protanopia, deuteranopia, or tritanopia, depending on whether the L, M, or S cone is defective, respectively [3]. Dichromatic vision is more common in males due to genetic characteristics. The proportion of dichromatic vision is about 25% for protanopia and 75% for deuteranopia. Tritanopia is relatively low at about 0.02%. Protanopia and deuteranopia are similar in color vision characteristics and have difficulty perceiving the difference among certain red and green colors.

(a) (b)

Fig. 1 Protanopia vision: (a) Original image, (b) Converted image to protanopia vision for (a).

Figure 1 shows an example of protanopia vision using Viénot et al.'s method [4]. From Fig. 1, we can see that it is difficult for protanopia vision to discriminate between flowers and leaves. Therefore, even color combinations that are easy to discriminate with trichromatic vision may not be discriminable with dichromatic vision.

Several image transformation methods have been proposed to convert images to facilitate color discrimination in dichromatic vision [5]–[14]. Kang et al. [9] proposed a color transformation method that uses the fact that the color discrimination range of dichromatic vision is represented by a plane [10]. This method transforms colors of an image by solving the optimization problem which maximizes a distance between colors on the dichromatic plane. Wang et al. [11] proposed a color conversion method by solving the optimization problem which maintains naturalness of an image and improves the contrast on the dichromatic plane. Though these methods generate the images whose colors can be discriminated by dichromatic vision, the impression of colors is significantly changed. Furthermore, the output images give an unnatural impression to trichromatic vision due to the change in hue.

Hassan and Paramesran's method [12] performs a color transformation that does not change the hue and lightness of image in the CIE XYZ color space. This method is a simple algorithm that does not require solving an optimization problem, but the visibility improvement effect for dichromatic vision is limited.

Tanaka et al.'s method [13] modifies the lightness of confusion color pairs which are chosen based on confusion lines. Dichromatic vision can discriminate colors which have

[†]The authors are with the Graduate School of Science and Technology for Innovation, Yamaguchi University, 1677–1 Yoshida, Yamaguchi-shi, Yamaguchi 753–8512, Japan

[††]The author is with the Graduate School of Science and Engineering, Kagoshima University, 1–21–40 Korimoto, Kagoshima-city, Kagoshima, 890–0065, Japan

[†††]The author is with the Faculty of Culture and Creative Arts, Yamaguchi Prefectural University, 3–2–1 Sakurabatake, Yamaguchi-shi, Yamaguchi 753–8502, Japan

Copyright © 200x The Institute of Electronics, Information and Communication Engineers

lightness differences because it perceives the same level of lightness with trichromatic vision. However, in this method, color pairs whose lightness are different in original images may be unnecessarily converted owing to choosing confusion color pairs without considering lightness differences. Meng and Tanaka [14] proposed a lightness conversion method which reflects a^* value of the CIE Lab color space in the lightness. Tanaka et al.'s method and Meng and Tanaka's method generate images that are easy for dichromatic vision to discriminate colors without losing the impression of original images, but the computational costs are high due to processing in the CIE Lab color space whose color gamut is complex.

In this paper, we propose an image transformation method to facilitate color discrimination for dichromatic vision by modifying only the lightness in the RGB color space without significantly changing the impression of original images. Concretely, the lightness modification is performed by adding the red-green component, which is calculated in the RGB color space and multiplied by a coefficient, to the lightness component. The coefficient is determined by solving a minimization problem for the lightness difference between pixels considering the color difference. Finally, hue and saturation are preserved before and after the lightness modification to produce an image that is easy to discriminate for dichromatic vision. The effectiveness of the proposed method is verified by experiments using various images.

The rest of this paper is organized as follows. Section 2 explains about the simulation of dichromatic vision. Section 3 describes the algorithm of the proposed method in detail. Section 4 shows the results of comparative experiments between the proposed method and conventional methods. Section 5 is devoted to the conclusion.

2. Simulation of dichromatic vision

Viénot et al. [4] proposed the method to simulate the view of dichromatic vision. The procedure for converting color image to dichromatic vision is described in [4], [15] and [16]. Let $E'_{8bit}(E \in \{R, G, B\})$ be the nonlinear RGB components in color images. Here, standard RGB (sRGB) is assumed as the RGB color space. The nonlinear RGB components E'_{sRGB} are first converted to the linear RGB components E_{sRGB} as follows:

$$E_{sRGB} = \begin{cases} E'_{sRGB}/12.92 & E'_{sRGB} \le 0.03928 \\ \left(\frac{E'_{sRGB}+0.055}{1.055}\right)^{2.4} & \text{otherwise} \end{cases}, \quad (1)$$

$$E'_{sRGB} = E'_{8bit}/255. \quad (2)$$

Next, the linear RGB components are converted to the XYZ components (X, Y, Z) as follows [17]:

$$\begin{pmatrix} X \\ Y \\ Z \end{pmatrix} = \begin{pmatrix} 0.4124 & 0.3576 & 0.1805 \\ 0.2126 & 0.7152 & 0.0722 \\ 0.0193 & 0.1192 & 0.9505 \end{pmatrix} \begin{pmatrix} R_{sRGB} \\ G_{sRGB} \\ B_{sRGB} \end{pmatrix}. \quad (3)$$

The conversion from the XYZ components to the LMS components, which represent the response in human cones, is expressed as follows [18]:

$$\begin{pmatrix} L \\ M \\ S \end{pmatrix} = \begin{pmatrix} 0.40024 & 0.70760 & -0.08081 \\ -0.22630 & 1.16532 & 0.04570 \\ 0.00000 & 0.00000 & 0.91822 \end{pmatrix} \begin{pmatrix} X \\ Y \\ Z \end{pmatrix}. \quad (4)$$

The LMS components for protanopia vision are given as follows:
when $M \ge S$,

$$\begin{pmatrix} L_P \\ M_P \\ S_P \end{pmatrix} = \begin{pmatrix} 0.00000 & 1.20800 & -0.20797 \\ 0.00000 & 1.00000 & 0.00000 \\ 0.00000 & 0.00000 & 1.00000 \end{pmatrix} \begin{pmatrix} L \\ M \\ S \end{pmatrix}, \quad (5)$$

and when $M < S$,

$$\begin{pmatrix} L_P \\ M_P \\ S_P \end{pmatrix} = \begin{pmatrix} 0.00000 & 1.22023 & -0.22020 \\ 0.00000 & 1.00000 & 0.00000 \\ 0.00000 & 0.00000 & 1.00000 \end{pmatrix} \begin{pmatrix} L \\ M \\ S \end{pmatrix}. \quad (6)$$

In protanopia vision, the coefficients of L in Eqs. (5) and (6) are 0 because the L cone is defective.

The LMS components for deuteranopia vision are given as follows:
when $L \ge S$,

$$\begin{pmatrix} L_D \\ M_D \\ S_D \end{pmatrix} = \begin{pmatrix} 1.00000 & 0.00000 & 0.00000 \\ 0.82781 & 0.00000 & 0.17216 \\ 0.00000 & 0.00000 & 1.00000 \end{pmatrix} \begin{pmatrix} L \\ M \\ S \end{pmatrix}, \quad (7)$$

and when $L < S$,

$$\begin{pmatrix} L_D \\ M_D \\ S_D \end{pmatrix} = \begin{pmatrix} 1.00000 & 0.00000 & 0.00000 \\ 0.81951 & 0.00000 & 0.18046 \\ 0.00000 & 0.00000 & 1.00000 \end{pmatrix} \begin{pmatrix} L \\ M \\ S \end{pmatrix}. \quad (8)$$

In deuteranopia vision, the coefficients of M in Eqs. (7) and (8) are 0 because the M cone is defective. Finally, by converting the LMS components in Eqs. (5)–(8) to the XYZ components and then converting them to the RGB components, the output image simulating the view of dichromatic vision can be obtained.

3. Proposed method

3.1 Minimization problem for lightness modification

In the proposed method, the modified lightness $\tilde{I}_i$ at pixel i is given as follows:

$$\tilde{I}_i = I_i + \tilde{c} x_{RG,i}, \quad (9)$$

where I_i is the lightness of pixel i and is given by the average of its RGB components. $x_{RG,i}$ indicates the red-green component of pixel i described later. The coefficient $\tilde{c}$ is given by solving the following minimization problem:

$$\tilde{c} = \arg\min_{c \in \mathbb{R}} \sum_{(i,j) \in \sigma_\rho} \left(\left(I'_i - I'_j \right) - \delta_{ij} \right)^2, \quad (10)$$

$$I'_i = I_i + c x_{RG,i}, \quad (11)$$

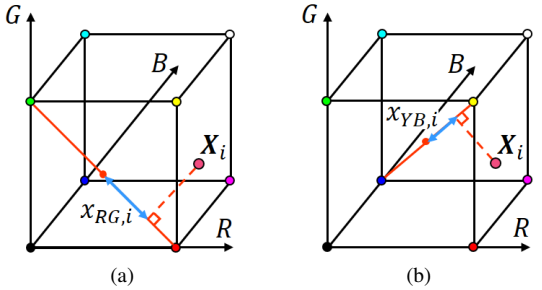

(a) (b)

Fig. 2 Examples of $x_{RG,i}$ and $x_{YB,i}$. (a) $x_{RG,i}$, (b) $x_{YB,i}$.

$$\delta_{ij} = (I_i - I_j) + \delta'_{ij}, \tag{12}$$

$$\delta'_{ij} = \mathrm{sign}(x_{RG,i} - x_{RG,j}) w_{ij} \Phi\left(\|\Delta C_{ij}\|\right), \tag{13}$$

$$w_{ij} = \exp\left(-\left(\frac{d_{ij}}{\beta}\right)^2\right), \tag{14}$$

$$\Phi(x) = \mu \tanh\left(\frac{x}{\mu}\right), \tag{15}$$

where I'_i, δ_{ij}, and δ'_{ij} are the lightness, the lightness difference and the lightness modification amount considering the difference in color, respectively. σ_ρ is the set of pixel pairs (i, j) that satisfy $d_c(i, j) \leq \rho$, where $d_c(i, j)$ is the chessboard distance between pixels i and j, and ρ is the neighborhood size. $\mathrm{sign}(x)$ is the sign of x. $\|\Delta C_{ij}\|$ is the color difference in trichromatic vision described later. β, μ are the parameters. w_{ij} is a weight defined by a Gaussian function of d_{ij}, where d_{ij} indicates the ease of discriminating between pixels i and j described later. A smaller value of d_{ij} indicates that pixels i and j are difficult to discriminate for dichromatic vision. Solving Eq. (10) using the least squares method yields the following $\tilde{c}$:

$$\tilde{c} = -\frac{\frac{1}{n}\sum_{(i,j)\in\sigma_\rho}\left(x_{RG,i} - x_{RG,j}\right)\left(I_i - I_j - \delta_{ij}\right)}{\frac{1}{n}\sum_{(i,j)\in\sigma_\rho}\left(x_{RG,i} - x_{RG,j}\right)^2}, \tag{16}$$

where n is the number of pixels.

Let $\boldsymbol{X}_i = (X_{R,i}, X_{G,i}, X_{B,i})$ be the RGB components at pixel i. We define the red-green and yellow-blue components $x_{RG,i}$ and $x_{YB,i}$ as follows:

$$x_{RG,i} = \frac{X_{R,i} - X_{G,i}}{\sqrt{2}} \tag{17}$$

and

$$x_{YB,i} = \frac{2X_{R,i} + 2X_{G,i} - 2X_{B,i} + 1}{2\sqrt{3}}, \tag{18}$$

respectively. $x_{RG,i}$ and $x_{YB,i}$ are the signed distances from the midpoints of the RG and YB straight lines in the RGB color space to the coordinates of the projections of a color coordinate onto these straight lines, respectively. Examples of $x_{RG,i}$ and $x_{YB,i}$ are shown in Fig. 2. $x_{RG,i}$ is close to red if positive and is close to green if negative. Similarly, $x_{YB,i}$ is close to yellow if positive and is close to blue if negative. Using $x_{RG,i}$ and $x_{YB,i}$, the color difference $\|\Delta C_{ij}\|$ in trichromatic vision is defined as follows:

$$\|\Delta C_{ij}\| = \sqrt{(x_{RG,i} - x_{RG,j})^2 + (x_{YB,i} - x_{YB,j})^2}. \tag{19}$$

The sign in Eq. (13) determines whether the lightness of pixel i or pixel j be enhanced and works to enhance the lightness of reddish colors more than that of greenish colors.

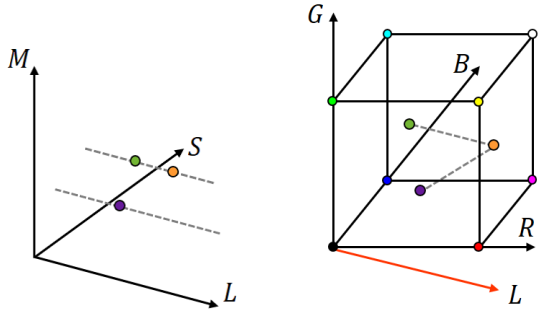

(a) (b)

Fig. 3 Color distribution in the LMS and RGB color spaces. (a) The LMS color space, (b) The RGB color space.

Next, we explain d_{ij} which represents the ease of color discrimination between pixels i and j. In the LMS color space, which is a three-dimensional color space with three types of cones response values as its axis, colors that are aligned parallel to the L-axis become difficult to discriminate for protanopia vision. Similarly, colors parallel to the M-axis are difficult to discriminate for deuteranopia vision. Figure 3 shows the color distribution in the LMS and RGB color spaces. Orange and green are difficult to discriminate in protanopia vision because they are aligned parallel to the L axis in the LMS color space. Since the LMS and RGB color spaces have a linear relationship, even in the RGB color space, these colors are distributed linearly and are parallel to the L axis. Using these characteristics of the distribution of colors that are difficult to discriminate in dichromatic vision, we define d_{ij} as follows:

$$d_{ij} = \gamma \|\boldsymbol{X}_{ij}\| f, \tag{20}$$

$$f = 1 - \left|\frac{\langle \boldsymbol{X}_{ij}, \boldsymbol{A}\rangle}{\|\boldsymbol{X}_{ij}\|\|\boldsymbol{A}\|}\right|, \tag{21}$$

$$\boldsymbol{X}_{ij} = \boldsymbol{X}_i - \boldsymbol{X}_j, \tag{22}$$

where $\boldsymbol{A}$ is a vector obtained by converting a certain axis of the LMS color space to the RGB color space and is represented by $\boldsymbol{A} \in \{\boldsymbol{L}, \boldsymbol{M}\}$. γ is a parameter to adjust the magnitude of d_{ij}. The operator $\langle\rangle$ represents the inner product. d_{ij} becomes smaller as the angle between $\boldsymbol{A}$ and $\boldsymbol{X}_{ij}$ decreases. In this case, pixels i and j become difficult to discriminate.

3.2 Hue and saturation preservation

In the proposed method, the lightness is modified while preserving the hue and saturation because of avoiding change of

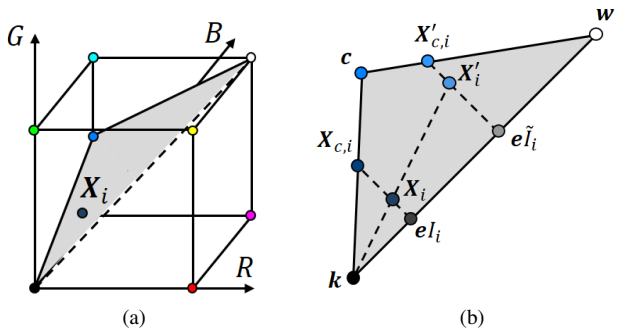

(a) (b)

Fig. 4 RGB color space and example of equi-hue plane. (a) RGB color space and pixel $\boldsymbol{X}_i$, (b) Equi-hue plane.

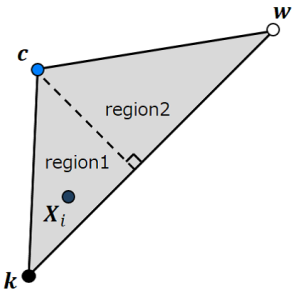

Fig. 5 Two regions divided on equi-hue plane.

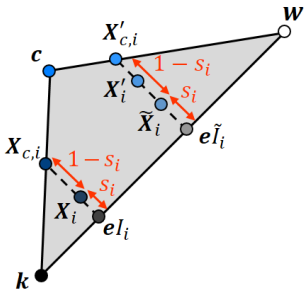

Fig. 6 Saturation preservation process.

the impression given by the original image. The RGB component $\boldsymbol{X}'_i$ after modifying the lightness is obtained using the lightness of the original image I_i and the modified lightness $\tilde{I}_i$ as follow:

$$\boldsymbol{X}'_i = \frac{\tilde{I}_i}{I_i}\boldsymbol{X}_i. \tag{23}$$

$\boldsymbol{X}'_i$ and $\boldsymbol{X}_i$ have the same hue because Eq. (23) satisfies the hue preserving condition defined by Naik and Murthy [19].

Next, the saturation preservation process is conducted on the equi-hue plane in the RGB color space [20]. Figure 4 shows the schematic diagram of the RGB color space and an example of the equi-hue plane. Figure 4(a) shows the RGB color space and the arbitrary pixel $\boldsymbol{X}_i$. The equi-hue plane is a triangle region which passes through white, black and $\boldsymbol{X}_i$. All points on the equi-hue plane have the same hue. Also, the line connecting white $\boldsymbol{w}$ and black $\boldsymbol{k}$ is called the achromatic axis, and the saturation of pixels on the line is 0. Figure 4(b) shows an example of the equi-hue plane. $\boldsymbol{X}_{c,i}$ is the most saturated color with the same lightness as the pixel $\boldsymbol{X}_i$. $\boldsymbol{e}I_i$ is a vector having the lightness of $\boldsymbol{X}_i$. $\boldsymbol{X}'_{c,i}$ is the most saturated color with the same lightness as the pixel $\boldsymbol{X}'_i$. $\boldsymbol{e}\tilde{I}_i$ is a vector having the modified lightness. $\boldsymbol{c}$ is the vertex of equi-hue plane except $\boldsymbol{w}$ and $\boldsymbol{k}$. In the proposed method, the saturation is defined as the ratio between the distance from the achromatic axis to $\boldsymbol{X}_i$ and the distance from the achromatic axis to $\boldsymbol{X}_{c,i}$. The following relationship holds among $\boldsymbol{X}_i$, $\boldsymbol{X}_{c,i}$ and the saturation s_i of $\boldsymbol{X}_i$:

$$\boldsymbol{X}_i = s_i\boldsymbol{X}_{c,i} + (1-s_i)\boldsymbol{e}I_i, \tag{24}$$

where $\boldsymbol{e}$ is the vector $\boldsymbol{e} = (1,1,1)$. The saturation s_i is calculated according to the region where $\boldsymbol{X}_i$ lies. If $\boldsymbol{X}_i$ is in region 1 shown in Fig. 5, then $\boldsymbol{X}_{c,i}$ is on the side $\boldsymbol{kc}$. Otherwise, $\boldsymbol{X}_{c,i}$ is on the side $\boldsymbol{wc}$. So, s_i should be calculated in each region. The border between the regions 1 and 2 is the perpendicular line from the vertex $\boldsymbol{c}$ to the achromatic axis, and the perpendicular line is included in the region 1. If $\boldsymbol{X}_i$ is in the region 1, $\boldsymbol{X}_{c,i}$ exists on side of $\boldsymbol{kc}$ and the minimum among RGB components of $\boldsymbol{X}_{c,i}$ is 0. If $\boldsymbol{X}_i$ is in the region 2, $\boldsymbol{X}_{c,i}$ exists on side of $\boldsymbol{wc}$ and the maximum among RGB components of $\boldsymbol{X}_{c,i}$ is 1. Therefore, the following equations hold:

$$\min\left(\boldsymbol{X}_{c,i}\right) = 0 \quad (\boldsymbol{X}_i \in \text{region1}) \tag{25}$$

and

$$\max\left(\boldsymbol{X}_{c,i}\right) = 1, \quad (\boldsymbol{X}_i \in \text{region2}) \tag{26}$$

where $\min\left(\boldsymbol{X}_{c,i}\right)$ and $\max\left(\boldsymbol{X}_{c,i}\right)$ are the minimum and the maximum among RGB components of $\boldsymbol{X}_{c,i}$, respectively. The following relationships hold among $\boldsymbol{X}_i$, $\boldsymbol{X}_{c,i}$ and s_i from Eq. (24):

$$\min(\boldsymbol{X}_i) = s_i \min(\boldsymbol{X}_{c,i}) + (1-s_i)\min(\boldsymbol{e})I_i \quad (\boldsymbol{X}_i \in \text{region1}) \tag{27}$$

and

$$\max(\boldsymbol{X}_i) = s_i \max(\boldsymbol{X}_{c,i}) + (1-s_i)\max(\boldsymbol{e})I_i. \quad (\boldsymbol{X}_i \in \text{region2}) \tag{28}$$

From Eqs. (25)–(28), the saturation s_i is calculated as follows:

$$s_i = \begin{cases} \dfrac{I_i - \min(\boldsymbol{X}_i)}{I_i}, & (\boldsymbol{X}_i \in \text{region1}) \\ \dfrac{I_i - \max(\boldsymbol{X}_i)}{I_i - 1}. & (\boldsymbol{X}_i \in \text{region2}) \end{cases} \tag{29}$$

Similarly, the saturation of $\boldsymbol{X}'_i$ calculated by Eq. (23) is obtained as follows:

$$s'_i = \begin{cases} \dfrac{\tilde{I}_i - \min(\boldsymbol{X}'_i)}{\tilde{I}_i}, & (\boldsymbol{X}'_i \in \text{region1}) \\ \dfrac{\tilde{I}_i - \max(\boldsymbol{X}'_i)}{\tilde{I}_i - 1}. & (\boldsymbol{X}'_i \in \text{region2}) \end{cases} \tag{30}$$

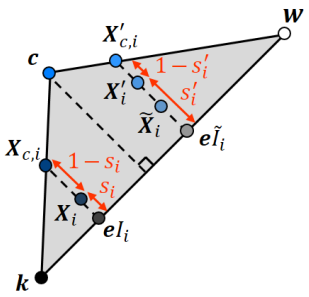

Fig. 7 Positional relationship of each point.

$\boldsymbol{X}'_i$ does not always preserve the saturation of the pixel $\boldsymbol{X}_i$. Figure 6 shows an example of the saturation preservation process. The RGB component $\tilde{\boldsymbol{X}}_i$, which is preserved the saturation of $\boldsymbol{X}_i$ and modified the lightness, is calculated as a vector divided internally $\boldsymbol{e}\tilde{\boldsymbol{I}}_i$ and $\boldsymbol{X}'_{c,i}$ by $s_i : 1 - s_i$ as follows:

$$\tilde{\boldsymbol{X}}_i = s_i \boldsymbol{X}'_{c,i} + (1 - s_i)\boldsymbol{e}\tilde{\boldsymbol{I}}_i. \tag{31}$$

$\boldsymbol{X}'_{c,i}$ can be calculated from the positional relationship of $\boldsymbol{X}'_i$ and $\boldsymbol{X}'_{c,i}$ as shown in Fig. 7. The following relationship holds among $\boldsymbol{X}'_i$, $\boldsymbol{X}'_{c,i}$, and s'_i:

$$\boldsymbol{X}'_i = s'_i \boldsymbol{X}'_{c,i} + (1 - s'_i)\boldsymbol{e}\tilde{\boldsymbol{I}}_i. \tag{32}$$

The most saturated point $\boldsymbol{X}'_{c,i}$ with lightness $\tilde{I}_i$ is obtained by rewriting Eq. (32) as follows:

$$\boldsymbol{X}'_{c,i} = \frac{\boldsymbol{X}'_i - (1 - s'_i)\boldsymbol{e}\tilde{\boldsymbol{I}}_i}{s'_i}. \tag{33}$$

According to Eq. (31), the output pixel value $\tilde{\boldsymbol{X}}_i$ is calculated from the obtained the saturation s_i and pixel value $\boldsymbol{X}'_{c,i}$. $\boldsymbol{X}'_i$ may be out of the color gamut of the RGB color space depending on the ratio between I_i and $\tilde{I}_i$. When the output pixel value $\tilde{\boldsymbol{X}}_i$ is calculated, $\boldsymbol{X}'_{c,i}$ and $\tilde{I}_i$ are used. Thus, it is guaranteed that the output pixel value $\tilde{\boldsymbol{X}}_i$ is in the color gamut.

4. Experiments

In experiments, a color chart and 104 natural images were used. Figure 8 shows the 104 natural images. As comparative methods, Tanaka et al.'s method [13], Hassan and Paramesran's method [12], Meng and Tanaka's methods [14], Kang et al.'s method [9], Wang et al.'s method [11] were used. In Kang et al.'s method, the parameter α was set to 1 to prioritize contrast improvement in dichromatic vision. The parameters in the other comparative methods were set to according to each reference. The parameters in the proposed method were set empirically as follows: $\beta = 0.6, \gamma = 0.6, \mu = 0.3, \rho = 10$. Viénot et al.'s method [4] was used to simulate the view of dichromatic vision.

4.1 Qualitative evaluation

In qualitative evaluation, the naturalness of colors and the ease of color discrimination in the resultant image are evaluated as the image quality. In particular, for resultant image of each method, a good result means an image which is not significantly changing the impression of the original image. Also, for converted image simulating dichromatic vision for the resultant image, a good result means an image which makes color combinations of original image that are difficult for dichromats to discriminate more distinguishable. Two examples of the result images are shown in Figs. 9, 10, 11, 12, and 13. These two images shown in Figs. 9 and 12 are named Image 1 and Image 2, respectively. Image 1 is the result for protanopia vision and Image 2 is the result for deuteranopia vision. Figures 9, 10, and 11 show the results for Image 1. Figure 10 shows the converted images to protanopia vision for the results of Image 1. Figure 11 shows the enlarged images from the green boxes in Fig. 10. As shown in Figs. 9(e) and 9(f), Kang et al.'s method and Wang et al.'s method change the color of the entire image. In the original image converted to protanopia vision shown in Fig. 10(a), it is difficult to discriminate red and green. As shown in Figs. 10(b)–10(g), all methods improve the visibility of red and green. From Figs. 11(b) and 11(d), Tanaka et al.'s method and Meng and Tanaka's method degrade the visibility of orange and yellow. In contrast, from Figs. 9(g), 10(g) and 11(g), the proposed method improves the visibility of red and green sufficiently without significantly changing the impression given by the original image and does not degrade the visibility of yellow and orange.

Figures 12 and 13 show the results for Image 2. Figure 13 shows the converted images to deuteranopia vision for the results of Image 2. From Figs. 12(e) and 12(f), Kang et al.'s method and Wang et al.'s method drastically change the color of the carrots. Also, the original image converted to deutetanopia vision shown in Fig. 13(a) is difficult to distinguish between orange and green. From Fig. 13(c), Hassan and Paramesran's method does not improve the visibility in deuteranopia vision. The images obtained by Kang et al.'s method and Wang et al.'s method show the unnatural color of the carrots or leaves. The other methods, including the proposed method, maintain the impression of the original image and improve the visibility in deuteranopia vision.

Next, the effectiveness of each method is verified by using a color chart. The images shown in the upper row of Fig. 14 are original image and resultant image, and the images shown in the lower row are converted images to protanopia vision. The color chart shown in the upper row of Fig. 14(a) consists of six pairs of colors. Each pair of colors is on the same confusion line in the xy chromaticity diagram. Each pair of colors is vertically arranged. The confusion lines consist of undiscriminatable colors for dichromatic vision in the xy chromaticity diagram. Pairs of colors on the same confusion line are considered indistinguishable in dichromatic vision. However, dichromatic vision can discriminate pairs of colors having lightness difference which are even on the same confusion line because the xy chromaticity diagram does not include lightness information. In the color chart shown in the upper row of Fig. 14(a), the pairs of columns

Fig. 8 List of images used in experiments.

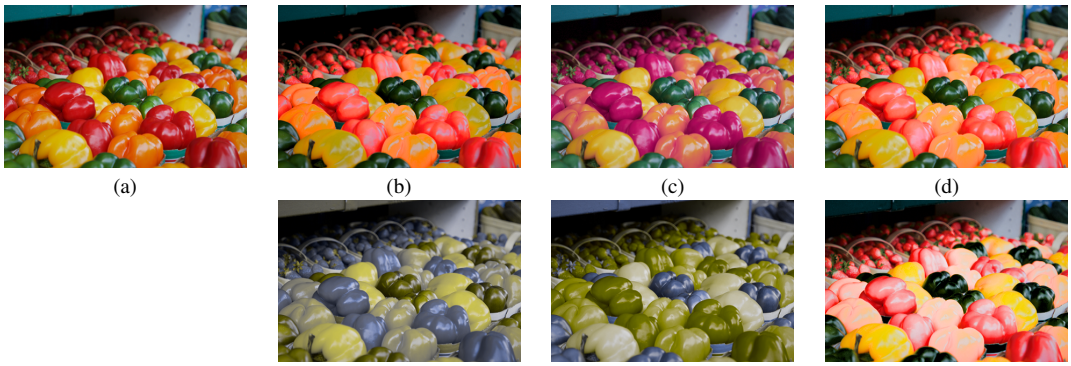

(a) (b) (c) (d) (e) (f) (g)

Fig. 9 The results of Image 1. (a) Original image, (b) Tanaka et al.'s method [13], (c) Hassan and Paramesran's method [12], (d) Meng and Tanaka's method [14], (e) Kang et al.'s method [9], (f) Wang et al.'s method [11], (g) Proposed method.

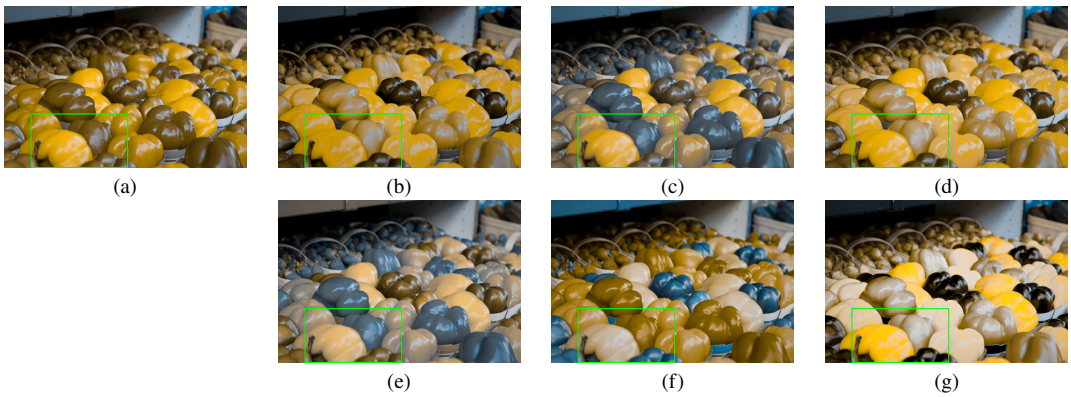

(a) (b) (c) (d) (e) (f) (g)

Fig. 10 Converted images to protanopia vision for the results of Image 1. (a) Original image, (b) Tanaka et al.'s method [13], (c) Hassan and Paramesran's method [12], (d) Meng and Tanaka's method [14], (e) Kang et al.'s method [9], (f) Wang et al.'s method [11], (g) Proposed method.

from 1 to 3 have sufficient lightness differences and the pairs of columns from 4 to 6 do not have lightness differences. In the color chart converted to protanopia vision shown in the lower row of Fig. 14(a), the pairs of columns from 1 to 3 can be discriminated by protanopia vision and the pairs of columns from 4 to 6 can not be discriminable. Figure 14 shows the results of the color chart. The images shown in the upper row of Fig. 14 are the original image and the result

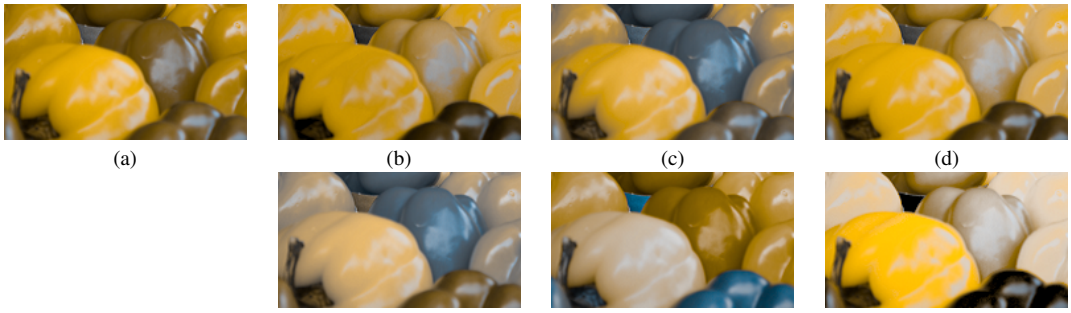

Fig. 11 Enlarged images of converted images to protanopia vision for the results of Image 1. (a) Original image, (b) Tanaka et al.'s method [13], (c) Hassan and Paramesran's method [12], (d) Meng and Tanaka's method [14], (e) Kang et al.'s method [9], (f) Wang et al.'s method [11], (g) Proposed method.

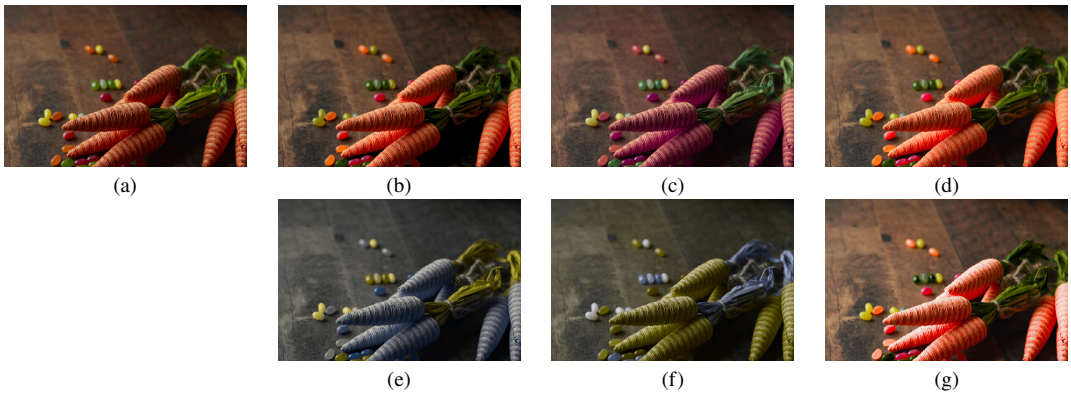

Fig. 12 The results of Image 2. (a) Original image, (b) Tanaka et al.'s method [13], (c) Hassan and Paramesran's method [12], (d) Meng and Tanaka's method [14], (e) Kang et al.'s method [9], (f) Wang et al.'s method [11], (g) Proposed method.

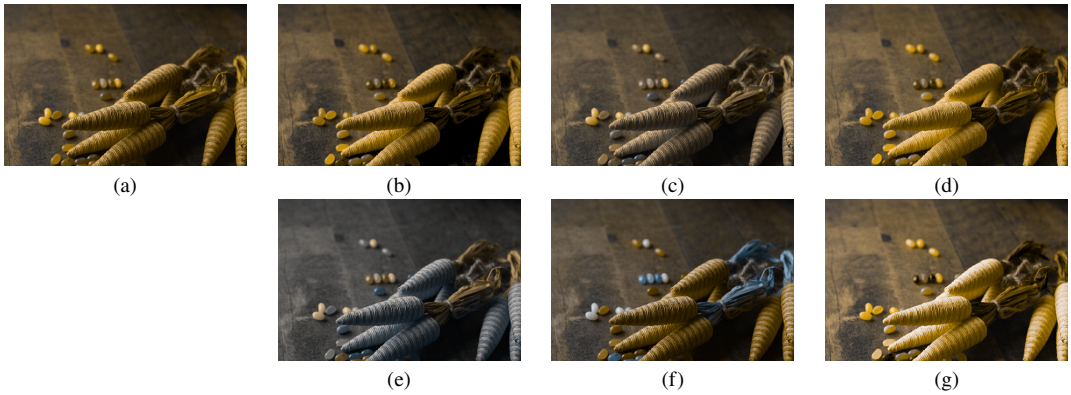

Fig. 13 Converted images to deuteranopia vision for the results of Image 2. (a) Original image, (b) Tanaka et al.'s method [13], (c) Hassan and Paramesran's method [12], (d) Meng and Tanaka's method [14], (e) Kang et al.'s method [9], (f) Wang et al.'s method [11], (g) Proposed method.

images, and the images of the lower row are the converted images to protanopia vision. From Figs. 14(c), 14(e) and 14(f), Hassan and Paramesran's method, Kang et al.'s method and Wang et al.'s method do not improve the visibility of the color pairs of columns from 4 to 6. Although Tanaka et al.'s method and Tanaka and Meng's method shown in Figs. 14(b) and 14(d) improve the visibility of the pairs of columns from 4 to 6, the pairs of columns from 1 to 3 are difficult to discriminate due to lightness conversion. As you can see from Fig. 14(g), the proposed method improves the visibility of the pairs of columns from 4 to 6 and does not degrade the visibility of the pairs of columns from 1 to 3.

4.2 Quantitative evaluation

In the quantitative evaluation, especially for the color chart,

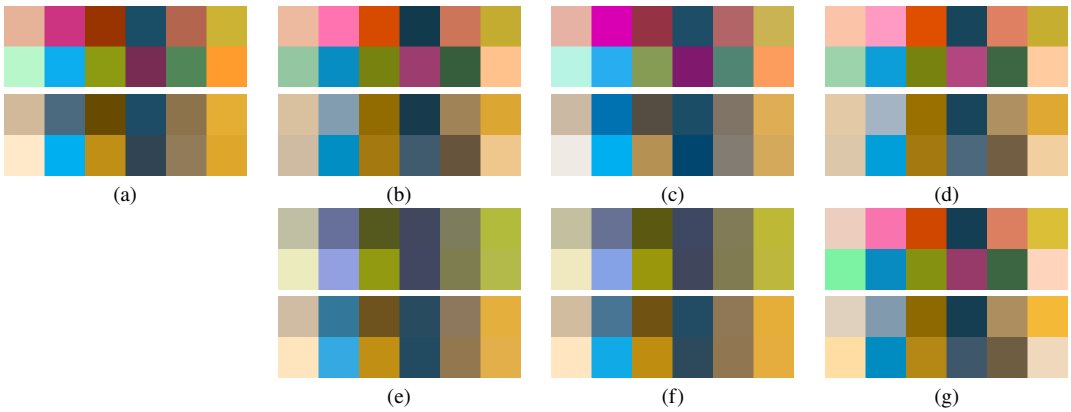

Fig. 14 The results of the color chart. The upper and lower rows represent resultant images and converted images to protanopia vision, respectively. (a) Original image, (b) Tanaka et al.'s method [13], (c) Hassan and Paramesran's method [12], (d) Meng and Tanaka's method [14], (e) Kang et al.'s method [9], (f) Wang et al.'s method [11], (g) Proposed method.

the color differences in each column are calculated. The color differences of the color chart are calculated for the color pairs of each column the converted images to protanopia vision shown in the lower row of Fig. 14. The color difference is defined as the Euclidean distance in the CIE Lab color space. Table 1 shows color differences of each column of the color pairs included in the converted images to protanopia vision shown in the lower row of Fig. 14. As shown in Table 1, in the original image, the color pairs of columns from 1 to 3 have large color differences and these colors can be discriminated as shown in Fig. 14. Also, the color pairs of columns from 4 to 6 have small color differences and these colors cannot be discriminated as shown in Fig. 14. From Table 1, Hassan and Paramesran's method, Kang et al.'s method and Wang et al.'s method generate small color differences for the column number from 4 to 6. In Tanaka et al.'s method and Meng and Tanaka's method, the color differences for the column number from 4 to 6 are larger than those of the original image, that is, these methods improve the visibility of the color pairs. However, these methods generate much smaller color differences for the column number 1 and 3 than those of the original image. For the color pairs of column number from 4 to 6, the proposed method increases the color differences from the original image and improves the visibility of them. For the color pairs of the column number from 1 to 3, the proposed method does not significantly decrease the color differences from the original image and does not degrade the visibility.

For the 104 natural images shown in Fig. 8, the evaluation is conducted using $\hat{V}$ [21]. In addition, processing time of each method is measured. The evaluation index $\hat{V}$ [21] is an index that evaluates the degree of contrast improvement for pixel pairs with lower contrast in dichromatic vision than in trichromatic vision:

$$\hat{V}_K = \frac{\hat{U}_K^{\text{out}}}{\hat{U}_K^{\text{in}}}, \tag{34}$$

$$\hat{U}_K^{\text{out}} = \frac{1}{|\sigma_K|} \sum_{(i,j)\in\sigma_K} |\hat{\lambda}_E \Delta\hat{E}_{K,ij}^{\text{out}} - \Delta E_{N,ij}^{\text{in}}|, \tag{35}$$

$$\hat{U}_K^{\text{in}} = \frac{1}{|\sigma_K|} \sum_{(i,j)\in\sigma_K} |\hat{\lambda}_E \Delta\hat{E}_{K,ij}^{\text{in}} - \Delta E_{N,ij}^{\text{in}}|, \tag{36}$$

$$\Delta\hat{E}_{K,ij}^{\text{out}} = \sqrt{\hat{\lambda}_{L^*}(\Delta L_{K,ij}^{*\text{out}})^2 + (\Delta a_{K,ij}^{*\text{out}})^2 + (\Delta b_{K,ij}^{*\text{out}})^2}, \tag{37}$$

$$\Delta\hat{E}_{K,ij}^{\text{in}} = \sqrt{\hat{\lambda}_{L^*}(\Delta L_{K,ij}^{*\text{in}})^2 + (\Delta a_{K,ij}^{*\text{in}})^2 + (\Delta b_{K,ij}^{*\text{in}})^2}, \tag{38}$$

$$\Delta E_{N,ij}^{\text{in}} = \sqrt{(\Delta L_{N,ij}^{*\text{in}})^2 + (\Delta a_{N,ij}^{*\text{in}})^2 + (\Delta b_{N,ij}^{*\text{in}})^2}. \tag{39}$$

Here, K represents the type of dichromatic vision, and $K \in \{P, D\}$. N represents trichromatic vision. $\hat{\lambda}_{L^*}$ and $\hat{\lambda}_E$ are the parameters. σ_K is the set of pixel pairs (i, j) that meet $d_c(i, j) \le \rho$ and $T_{K,ij} \le \tau$, where ρ and τ are the parameters. $d_c(i, j)$ is the chessboard distance mentioned above. $T_{K,ij}$ is defined as follows:

$$T_{K,ij} = \Delta E_{K,ij}^{\text{in}} / \Delta E_{N,ij}^{\text{in}}, \tag{40}$$

$$\Delta E_{K,ij}^{\text{in}} = \sqrt{(\Delta L_{K,ij}^{*\text{in}})^2 + (\Delta a_{K,ij}^{*\text{in}})^2 + (\Delta b_{K,ij}^{*\text{in}})^2}. \tag{41}$$

In the calculation of $\hat{V}$, we set $\rho = 5, \tau = 0.4, \hat{\lambda}_E = 0.3, \hat{\lambda}_{L^*} = 9$. When $\hat{V}$ is closer to 0, the contrast in dichromatic vision is similar to that in trichromatic vision, indicating better results.

Figures 15 and 16 show $\hat{V}_P$ and $\hat{V}_D$ results of each method for the 104 natural images. As you can see from Figs. 15 and 16, the averages of $\hat{V}_P$ and $\hat{V}_D$ of the proposed method are comparable to those of Meng and Tanaka's method, and the proposed method stably provides better results in protanopia and deuteranopia visions.

Table 2 shows the average processing times when the comparative and proposed methods are applied to the natural images of 300 × 300 pixels using Core™i7-6950 3.00GHz, RAM 32.0GB. The programming language is MATLAB R2019a. Since the proposed method uses the RGB color space, it is faster than Tanaka et al.'s method and Meng and Tanaka's method. Hassan and Paramesran's method, Kang

Table 1 Color differences between the colors in each column of the color chart.

Column number	1	2	3	4	5	6
Original image	17.01	37.29	35.26	9.17	4.50	2.25
Tanaka et al.	4.72	25.53	5.51	14.59	22.26	30.88
Hassan and Paramesran	19.41	24.72	41.46	9.91	4.33	7.24
Meng and Tanaka	3.93	34.01	3.21	15.59	23.31	38.50
Kang et al.	16.63	22.14	39.09	1.67	8.61	5.66
Wang et al.	15.27	27.75	35.01	3.76	2.40	2.71
Prop.	22.59	25.83	14.57	11.87	23.23	53.71

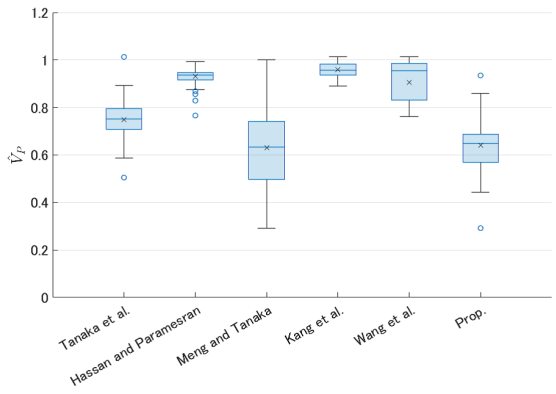

Fig. 15 Results of $\hat{V}_P$ for each method.

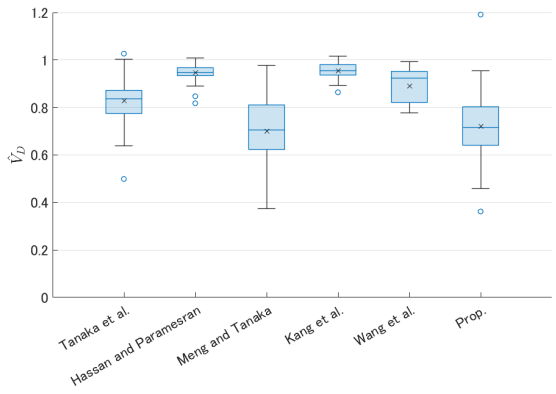

Fig. 16 Results of $\hat{V}_D$ for each method.

Table 2 Processing time. [sec.]

	Ave.	Std. Dev.
Tanaka et al.	48.26	22.58
Hassan and Paramesran	0.16	0.007
Meng and Tanaka	22.89	0.24
Kang et al.	1.69	0.017
Wang et al.	0.11	0.021
Prop.	4.40	0.040

et al.'s method, and Wang et al.'s method are faster than the proposed method, but in the quantitative evaluation mentioned above, the proposed method provides better results.

5. Conclusion

In this paper, we proposed a method to convert the original image into the image that was easy for dichromatic vision to discriminate colors without significantly changing the impression given by the original image for trichromatic vision, by modifying only the lightness in the RGB color space. Experimental results showed that the proposed method could improve the visibility of colors that were difficult to discriminate by appropriately modifying the lightness of the colors.

Future works are to further improve the quality of resulting images by refining the parameters and to reduce computational costs.

References

[1] G. Sharma, Digital Color Imaging Handbook, CRC Press, 2002.
[2] C. L. Hardin and L. Maffi, Color Categories in Thought and Language, Cambridge University Press, 1997.
[3] P. Gouras, The Perception of Colour, Macmillan Press, Scientific & Medical, 1991.
[4] F. Viénot, H. Brettel, and J.D. Mollon, "Degital video colourmaps for checking the legibility of displays by dichromats," Color Research & Application, vol.24, no.4, pp.243–252, Aug. 1999.
[5] G. Tanaka, N. Suetake, and E. Uchino, "Yellow-blue component modification of color image for protanopia or deuteranopia," IEICE Trans. on Fundamentals, vol.94-A, no.2, pp.884–888, Feb. 2011.
[6] N. Suetake, G. Tanaka, H. Hashii, and E. Uchino, "Simple lightness modification for color vision impaired based on Craik-O'Brien effect," Journal of the Franklin Institute, vol.349, no.6, pp.2093–2107, Mar. 2012.
[7] S. Bao, G. Tanaka, H. Tamukoh, and N. Suetake, "Lightness modification method considering Craik-O'Brien effect for protanopia and deuteranopia," IEICE Trans. on Fundamentals, vol.E99-A, no.11, pp.2008–2011, Nov. 2016.
[8] H. Orii, H. Kawano, N. Suetake, and H. Maeda, "Color conversion for color blindness employing multilayer neural network with perceptual model," Image and Video Technology, 7th Pacific-Rim Symposium, pp.3–14, 2016.
[9] S.-K. Kang, C. Lee, and C.-S. Kim, "Optimized color contrast enhancement for dichromats using local and global contrast," Proc. of the IEEE Int. Conf. Image Process., pp.1048–1052, 2020.
[10] G. R. Kuhn, M. M. Oliveira, and L. A. F. Fernandes, "An efficient naturalness-preserving image-recoloring method for dichromats," IEEE Trans. Vis. Comput. Graph, vol. 14, no. 6, pp. 1747–1754, Nov. 2008.
[11] X. Wang, Z. Zhu, X. Chen, K. Go, M. Toyoura, and X. Mao, "Fast contrast and naturalness preserving image recolouring for dichromats," Computer&Graphics, vol.98, pp.19–28, Aug. 2021.
[12] M. F. Hassan and R. Paramesran, "Naturalness preserving image recoloring method for people with red-green deficiency," Signal Processing: Image Communication, vol.57, pp.126–133, Sep. 2017.
[13] G. Tanaka, N. Suetake, and E. Uchino, "Lightness modification of color image for protanopia and deuteranopia," Optical Review, vol.17, no.1, pp.14–23, Jan. 2010.
[14] M. Meng and G. Tanaka, "Proposal of minimization problem based lightness modification method considering visual characteristics of

protanopia and deuteranopia," Proc. Asia-Pacific Signal and Information Processing Association Annual Summit and Conf. 2019, pp.1417–1422, 2019.
[15] H. Brettel, F. Viénot, and J.D. Mollon, "Computerized simulation of color appearance for dichromats," J. Opt. Soc. Am. A, vol.14, no.10, pp.2647–2655, Oct. 1997.
[16] Kazunori Asada: Official Website "Chromatic Vision Simulator" `https://asada.website/webCVS/`. Accessed 14 Feb. 2024.
[17] IEC 61966-2-1. Multimedia Systems and Equipment -Colour measurement and management- Part 2-1: Colour Management -Default RGB Colour Space- sRGB, 1999.
[18] R.W.G. Hunt and M.R. Pointer, Measuring Colour, 4th ed., Wiley. Chichester, UK, 2013.
[19] S. K. Naik and C. A. Murthy, "Hue-preserving color image enhancement without gamut problem," IEEE Trans. Image Process., vol.12, no.12, pp.1591–1598, Dec. 2003.
[20] D. Moriyama, Y. Ueda, H. Misawa, N. Suetake and E. Uchino, "Saturation-based multi exposure image fusion employing local color correction," Proc. of the IEEE Int. Conf. Image Process., pp.3512–3516, 2019.
[21] X. Cheng and G. Tanaka, "A novel quantitative evaluation index of contrast improvement for dichromats," IEICE Trans. Fundamentals, vol.E103-A, no.12, pp.1618–1620, Dec. 2020.

Ayaka Fujita received the B.S. and M.S. degrees in science from Yamaguchi University, Japan, in 2022 and 2024, respectively. She is currently pursuing the Ph.D. degree at the Graduate School of Sciences and Technology for Innovation, Yamaguchi University, Japan. Her research interests include image processing. She is a member of IEICE and IEEE.

Mashiho Mukaida received the M.S. and Ph.D. degrees from Yamaguchi University, Japan, in 2021 and 2024, respectively. He is currently with the Graduate School of Science and Engineering, Kagoshima University, Japan, where he is an associate professor. His research interests include image processing. He is a member of the IEICE and IEEE.

Tadahiro Azetsu received the B.S., M.S. and Ph.D. degrees in science from Yamaguchi University, Japan, in 1994, 1996 and 2007, respectively. He is currently with the Department of Culture and Creative Arts, Yamaguchi Prefectural University, Japan, where he is a professor. His research interests include image processing and speech signal processing. He is a member of IEICE.

Noriaki Suetake received the B.E., M.E., and Ph.D. degrees in control engineering and science from the Kyushu Institute of Technology, Japan, in 1992, 1994, and 2000, respectively. He is currently with the Graduate School of Sciences and Technology for Innovation, Yamaguchi University, Japan, where he is a Professor. His research interests include digital signal processing, image processing, and intelligent systems. He is a member of the IEICE, IEEE and OPTICA.